Journal of Catalysis 261 (2009) 88–93

Contents lists available at ScienceDirect

Journal of Catalysis

www.elsevier.com/locate/jcat

Magnetically separable Pt catalyst for asymmetric hydrogenation

Barbara Panella, Angelo Vargas, Alfons Baiker *

Institute for Chemical and Bioengineering, Department of Chemistry and Applied Biosciences, ETH Zürich, Hönggerberg, Wolfgang-Pauli-Str. 10, CH-8093 Zürich, Switzerland

ARTICLE INFO

Article history:
Received 20 September 2008
Revised 3 November 2008
Accepted 4 November 2008
Available online 28 November 2008

Keywords:
Superparamagnetic nanoparticles
Magnetic properties
Magnetite
Enantioselective hydrogenation
Asymmetric catalysis
Platinum
Cinchonidine
Catalyst recycling

ABSTRACT

A magnetic $Pt/SiO_2/Fe_3O_4$ catalyst consisting of chirally modified platinum supported on silica coated magnetite nanoparticles was prepared using an easy synthetic route and successfully applied for the enantioselective hydrogenation of various activated ketones. The magnetic catalyst modified with cinchonidine showed a catalytic performance (activity, enantioselectivity) in the asymmetric hydrogenation of various activated ketones in toluene comparable to the best known Pt/alumina catalyst used for these reactions. The novel catalyst can be easily separated from the reaction solution by applying an external magnetic field and recycled several times with almost complete retention of activity and enantioselectivity.

1. Introduction

Catalyst separation and recycling are essential steps in catalytic technology and frequently affect the overall process economy. A possible solution to facilitate this step is the use of solid catalysts with magnetic properties which can be efficiently separated from the reaction medium applying an external magnetic field [1–6]. In particular magnetic particles in the nanometer range are superparamagnetic and have therefore exceptional properties, suitable both for catalytic reactions in solution and for magnetic recovery. On the one hand, superparamagnetic particles are intrinsically non-magnetic above the so-called blocking temperature and have therefore no tendency to aggregate in solution allowing optimal mixing conditions for catalytic reactions. On the other hand, these nanoparticles are readily magnetized by an external magnetic field which favors their separation from the reaction solution. The approach of using magnetically recoverable catalysts has been recently followed by supporting a metal catalyst on a magnetic support, for example in decarboxylative coupling [7], olefin epoxidation [8], and hydrogenation reactions [9–11]. In the field of asymmetric hydrogenation reactions, to the best of our knowledge, the only example of magnetic separation is the immobilization of a homogeneous asymmetric ruthenium catalyst on magnetic nanoparticles [12]. In this approach the precious catalyst, which is active in the hydrogenation of aromatic ketones, was chemically bound to magnetic SiO_2/Fe_3O_4 nanoparticles, and thus separated and reused after the reaction.

The present investigation deals with a different approach to asymmetric hydrogenation [13–17]: the well known technique of chiral surface modification by means of cinchona alkaloids is coupled with the use of a magnetic support thus obtaining a truly heterogeneous rather than an immobilized homogeneous-type catalyst. We prepared and structurally characterized a magnetic chirally modified Pt catalyst for the enantioselective hydrogenation of activated ketones and compared its catalytic behavior with that of one of the best known commercial Pt/alumina catalysts applied for this kind of reactions. The recyclability of the novel catalyst was tested by performing several magnetic separations and reactions without further activation of the catalyst.

2. Experimental

2.1. Materials

For the preparation of the catalyst ferric chloride hexahydrate (>99%) and ferrous chloride tetrahydrate (>99%) purchased from Aldrich were used. Sodium silicate powder was purchased from Fisher Scientific AG and platinum (II) acetylacetonate from ABCR. Cinchonidine (CD, ⩾98%) was purchased from Fluka and acetic acid (99.8%) from Acros Organics. Toluene from Fluka (⩾99.7%) was dried over molecular sieve 4A. The substrates α,α,α-trifluoroacetophenone (Fluka, ⩾98%), ethyl pyruvate (Acros Organics, ⩾98%), ketopantolactone (DSM Nutritional Products AG) and

---

* Corresponding author. Fax: +41 44 6321163.
E-mail address: baiker@chem.ethz.ch (A. Baiker).

0021-9517/$ – see front matter © 2008 Elsevier Inc. All rights reserved.
doi:10.1016/j.jcat.2008.11.002

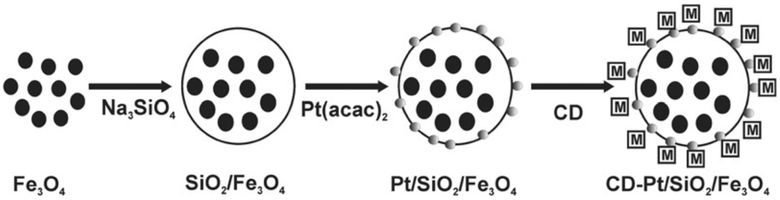

Fig. 1. Preparation of the magnetic, chirally modified $Pt/SiO_2/Fe_3O_4$ (M represents cinchonidine).

methylbenzoylformate (Acros Organics, 99%) were used without further purification.

2.2. Catalyst preparation

The magnetite nanoparticles were prepared by coprecipitation according to the synthesis reported by Liu et al. [18]: 11.67 g of $FeCl_3 \cdot 6H_2O$ and 4.3 g $FeCl_2 \cdot 4H_2O$ were dissolved in 200 ml of distilled water. The solution was stirred under constant nitrogen gas flow and heated up at 85 °C. Subsequently 15 ml of 25% $NH_3 \cdot H_2O$ were added to the solution which immediately became dark brown indicating the formation of the magnetite particles. The solution was stirred for further 30 min at 85 °C under inert atmosphere. After cooling down to room temperature the magnetic nanoparticles were separated from the water solution. 47.50 g of sodium silicate were dissolved in 400 ml of distilled water and the pH was adjusted to $pH = 12–13$ using hydrochloric acid. Since the solution was not completely clear the non-dissolved sodium silicate was filtered off. The magnetic particles were added to the silicate solution which was stirred mechanically and heated to 80 °C. The pH of the solution was slowly adjusted to $pH = 6–7$ by adding dropwise under stirring a solution of 37% HCl dissolved in the same volume of water. The silica coated magnetic nanoparticles were filtered off and the coating procedure was repeated. The $Pt/SiO_2/Fe_3O_4$ catalyst was prepared by incipient wetting impregnation. 9.4 g of the silica coated magnetite particles were dried in air at 80 °C for 4 h. 1.02 g of platinum (II) acetylacetonate was dissolved in the minimum quantity of toluene necessary for dissolution. The solution was added dropwise to the dried silica coated magnetic nanoparticles under vigorous stirring until the solid had a sticky appearance. Then the solid was dried in air at 100 °C. The procedure was repeated several times. At the end the solid was dried at 100 °C over night and then calcined at 400 °C for approximately 2 h. The solid was then pressed in pellets which were crushed and sieved to obtain particles with a size between 100 µm and 200 µm. The catalyst preparation route is schematically shown in Fig. 1.

A commercial 5 wt% Pt/alumina catalyst (Engelhard 4759) served as a reference for the catalytic tests. Characteristic properties of this catalyst which has been frequently applied in the enantioselective hydrogenation over cinchona-modified platinum have been specified in Refs. [19,20].

2.3. Catalyst characterization

The nitrogen adsorption isotherm of the magnetic catalyst was measured at 77 K with a Micromeritics ASAP 2000 apparatus after degassing the sample at 80 °C in vacuum for 2 h. The multipoint BET specific surface area was obtained in the p/p_0 range of 0.05–0.3.

The XRD pattern of the samples were recorded with a Siemens D5000 powder X-ray diffractometer using Cu $K\alpha$ radiation in the range of $15^\circ < 2\theta < 65^\circ$ and a step size of 0.01°.

The platinum content was determined using a SpectrAA Varian atomic absorption spectrometer after dissolving the supported platinum in aqua regia. Atomic absorption was also applied to determine potential leaching of iron into solution during hydrogenation.

The magnetic measurements were performed with a superconducting quantum interference device (SQUID MPMS-XL) at room temperature and 5 K.

For transmission electron microscopy (TEM), the catalyst material was dispersed in ethanol and deposited onto a perforated carbon foil supported on a copper grid (Okenshoji Co. Ltd.). The microscope (Tecnai 30F FEI with a field emission cathode, operated at 300 kV) was also equipped with a high angle annular dark-field (HAADF) detector for scanning transmission electron microscopy showing the metal particles with bright contrast (Z contrast). For qualitative analysis, the electron beam was set to selected areas in the scanning transmission electron microscopy (STEM) images and the signal was measured by energy dispersive X-ray spectroscopy (EDXS; detector: EDAX).

Attenuated total reflection–infrared spectroscopy measurements were performed with a home-build stainless steel batch reactor cell equipped with a mechanical stirrer and possessing a ZnSe crystal window at the bottom used as internal reflection element. The cell, which was kept at a constant temperature of 298 K with a thermostat, was mounted on the optical bench of a FT-IR spectrometer (Bruker Optics Equinox 55) equipped with a MCT detector cooled with liquid nitrogen. The ATR-IR spectra were recorded by averaging 100 scans at a resolution of 4 cm^{-1}.

2.4. Hydrogenation reactions

For the enantioselective hydrogenation the catalyst was treated at 250 °C under nitrogen flow for 30 min, followed by reduction at 250 °C in H_2 flow for 2 h and cooling down to room temperature in H_2 flow. The commercial Pt/Al_2O_3 catalyst was activated with a standard procedure [19]: heating at 400 °C under N_2 flow for 30 min, reduction at the same temperature under H_2 flow for 1 h and then cooling to RT in H_2. For the reaction at 11 bar, 42 mg of catalyst, 5 ml of toluene, 2 mg of cinchonidine (CD) and 1.85 mM of substrate were stirred at 1000 rpm in a parallel pressure reactor system Endeavor^{TM} with eight mechanically stirred reactors. For recycling the catalyst was magnetically separated and washed twice with toluene and the reaction was repeated under the same conditions as described above. The enantiomeric excess is expressed as $ee\ (\%) = [|(R - S)|/(R + S)] \cdot 100$ and the error in ee values is calculated as standard deviation of four distinct measurements and corresponds to $\sigma_{ee} = (1–3)\%$. The products were identified by GC on a Thermo Finnigan Trace 2000 using a CP-Chirasil-Dex CB capillary column and a FID detector. The high pressure reaction was performed under the same conditions but at 100 bar and in a stainless steel batch reactor equipped with a glass liner.

For conversion and recycling measurements 13 mg of catalyst, 2 mg of CD and 3.7 mM of substrate ketopantolactone (KPL, dihydro-4,4-dimethyl-2,3-furandione) were used. The error bars in this case are calculated as the difference in the values of two distinct measurements.

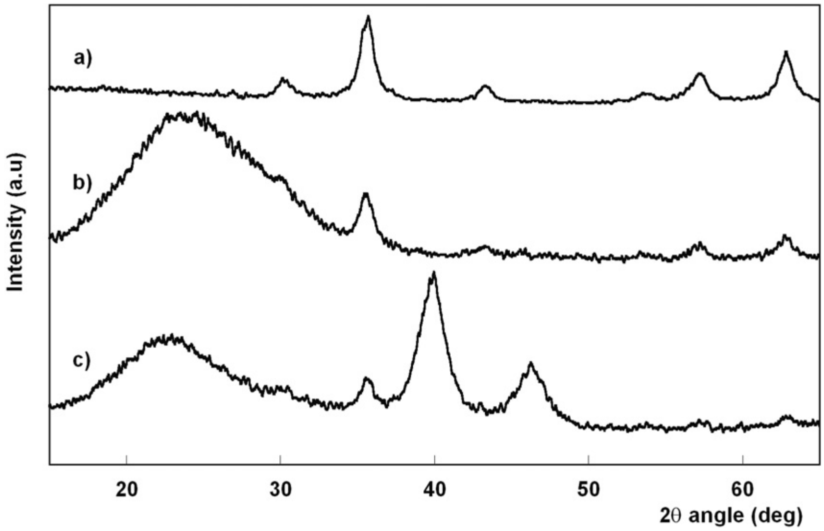

Fig. 2. XRD pattern of (a) magnetite nanoparticles prepared by coprecipitation, (b) silica coated magnetite nanoparticles, (c) the pretreated Pt/SiO_2/Fe_3O_4 catalyst.

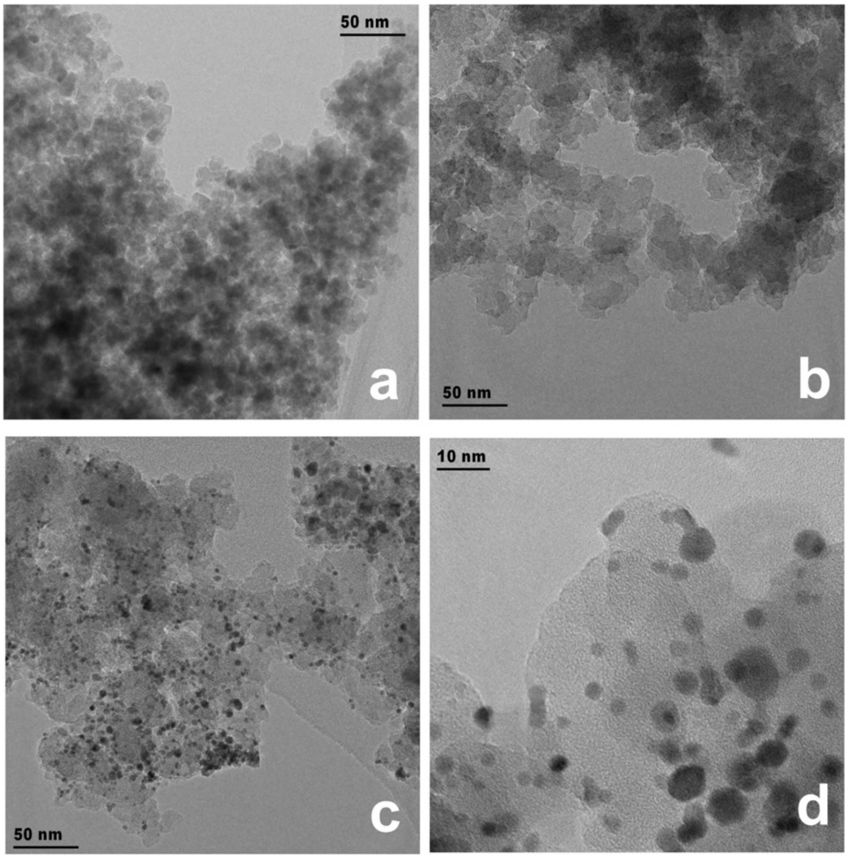

Fig. 3. TEM images of (a) magnetite nanoparticles, (b) silica coated magnetite nanoparticles, (c, d) the Pt/SiO_2/Fe_3O_4 catalyst.

3. Results and discussion

3.1. Structural and magnetic properties of catalyst

Figs. 2a and 3a show the XRD pattern and the TEM images, respectively, of the as-prepared iron oxide nanoparticles. The XRD pattern correspond well to the reflections of magnetite (Fe_3O_4), even though the presence of γ-Fe_2O_3 cannot be excluded due to the very close position of the reflections for the two similar structures. The mean particle size of the magnetite particles determined from the line broadening of the (311) reflection of Fe_3O_4 at 35.69° using the Scherrer formula corresponds to approximately 8 nm. Similarly, TEM images show particles with an average size of ∼10 nm (Fig. 3a). However, the particles are not uniform in size, their diameter ranges between 6 to 14 nm. In the XRD pattern of the silica coated magnetic particles both the reflections of magnetite and a broad maximum assigned to amorphous silica at $2\theta \approx 24°$ can be observed which indicate that the structure of the magnetite was maintained after the silica coating. The SiO_2/Fe_3O_4 particles do not show an ordered core–shell structure with a magnetic core and a spherical silica coating (Fig. 3b). High angle annular dark-field scanning transmission electron mi-

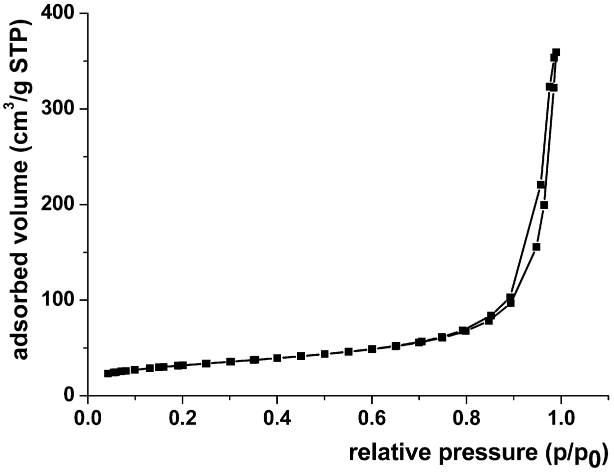

Fig. 4. Nitrogen adsorption isotherm of the magnetic $Pt/SiO_2/Fe_3O_4$ catalyst.

croscopy (HAADF-STEM) combined with energy dispersive X-ray analysis showed that their structure is better described as a dispersion of larger agglomerates of magnetic Fe_3O_4 nanoparticles in a silica matrix. The average Si:Fe atomic ratio of the composite material, as determined by ICP-OES was approximately 14:1. After platinum deposition and reduction with hydrogen the XRD pattern of the catalyst additionally showed the (111) and (200) reflections of metallic platinum (Fig. 2c). No formation of metallic iron was observed after reduction in hydrogen. The platinum particles had a mean size of 4.4 nm, as determined using the Scherrer formula which matches well with the mean size (5 ± 2 nm) determined from the TEM images (Figs. 3c and 3d). The nitrogen adsorption isotherm of the (5.2 ± 0.1) wt% $Pt/SiO_2/Fe_3O_4$ catalyst showed a type II shape with a very weak hysteresis (Fig. 4). This type of isotherm is characteristic for non-porous or macroporous materials and the small hysteresis loop is attributed to the interparticle void space rather than to some mesoporosity of the sample. The BET specific surface area of the as-prepared $Pt/SiO_2/Fe_3O_4$ catalyst was 111 m^2/g. The commercial 5 wt% Pt/Al_2O_3 catalyst (Engelhard 4759), which was used as a reference for comparison with the newly designed catalyst, possesses a BET specific surface area of 168 m^2/g and a mean platinum particle size of 4.5 nm [20].

Fig. 5 shows the magnetization curves of the as prepared magnetite nanoparticles (a) and of the $Pt/SiO_2/Fe_3O_4$ catalyst (b) at 300 K and 5 K. At room temperature both show only a negligible coercivity (H_c) (Table 1), which is characteristic for the superparamagnetic behavior of nanoparticles. For these particles the saturation magnetization (M_s) at 4 T is approximately 4 $emu\,g^{-1}$. At 5 K the coercivity increases since the thermal energy is smaller than the anisotropy energy.

3.2. Separation, catalytic behavior and recyclability

The magnetic catalyst could be easily separated from a toluene solution with a magnet, and showed no tendency to self-aggregation thus forming a stable suspension (Fig. 6). This is due to the superparamagnetic properties of the nanoparticles in the support which do not retain the magnetization in absence of an external magnetic field. Furthermore, the protective silica coating, even in case of a small residual permanent magnetization reduces the anisotropic magnetic dipolar attraction between the particles [18,21,22]. The silica coating has also the function to avoid the encapsulation of Pt particles into Fe_3O_4 since it prevents the exposure of magnetite particles on the surface [23].

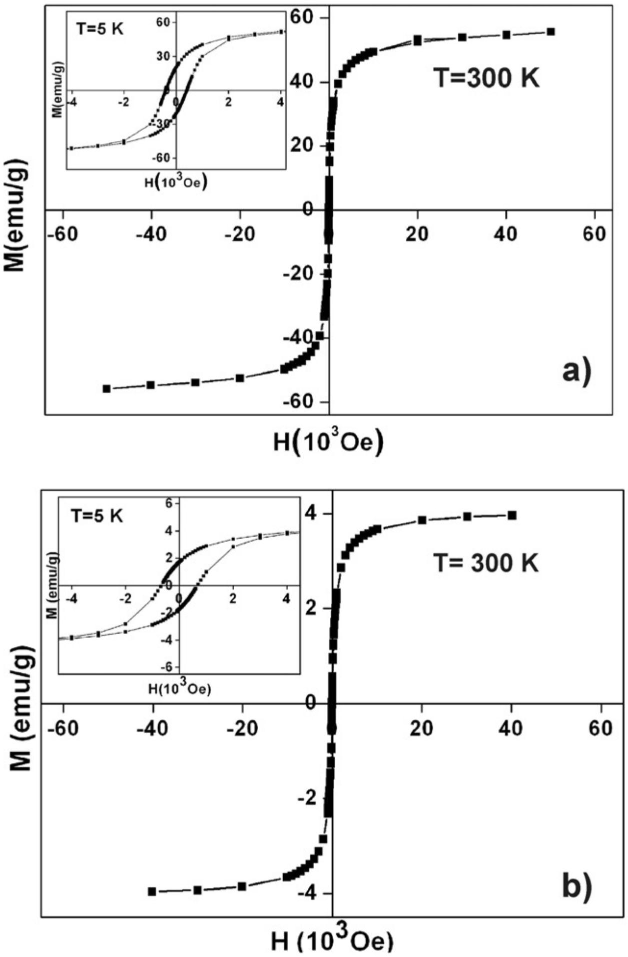

Fig. 5. Magnetization curve (a) of the magnetite nanoparticles at 300 K and 5 K (in the inset) and (b) of the $Pt/SiO_2/Fe_3O_4$ catalyst at 300 K and 5 K (in the inset).

Table 1
Magnetic properties (saturation magnetization, M_s; coercivity, H_c) of the magnetite nanoparticles and of the magnetic $Pt/SiO_2/Fe_3O_4$ catalyst.

	M_s (emu/g)	H_c (Oe)
Fe_3O_4		
300 K	55.5	8
5 K	63.9	404
$Pt/SiO_2/Fe_3O_4$		
300 K	4.0	4
5 K	5.2	682

The 5.2 wt% $Pt/SiO_2/Fe_3O_4$ catalyst was applied for the enantioselective hydrogenation of α-ketoesters and α,α,α-trifluoroacetophenone using CD as surface modifier and its catalytic performance was compared to that of the commercial 5 wt% Pt/alumina catalyst (Engelhard 4759) used as a reference. This catalyst is a standard commercial catalyst used for enantioselective hydrogenation of α-ketoesters in heterogeneous catalysis [13,20]. The results of these comparative catalytic tests are summarized in Table 2.

The hydrogenation of the various activated ketones using $Pt/SiO_2/Fe_3O_4$ was performed under standard conditions [24] in toluene at room temperature and 11 bar of H_2. For all substrates the conversion was complete after a maximum reaction time of 2 h. The enantiomeric excess (ee) values obtained for the first run with the magnetic catalyst are comparable to those obtained under the same conditions with the Pt/Al_2O_3 reference catalyst. An exception was the hydrogenation of methylbenzoylformate where a 13% lower ee was obtained for the $Pt/SiO_2/Fe_3O_4$ catalyst. Considering the high sensitivity of the catalyst performance on texture, metal-dispersion and composition in cinchona modified systems, the good catalytic performance achieved with the novel magnetic

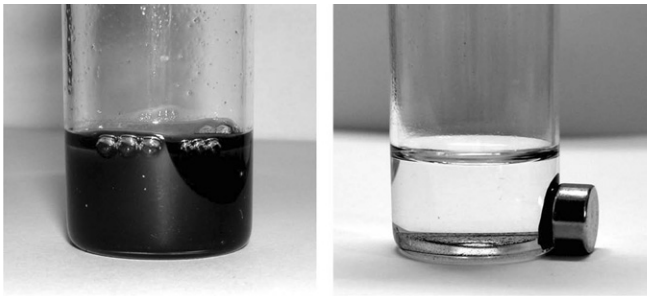

Fig. 6. The $Pt/SiO_2/Fe_3O_4$ catalyst is homogeneously suspended in toluene, when stirred (left) and can be easily separated from the solution with a magnet (right).

Table 2
Enantiomeric excess (ee) achieved at full conversion in the hydrogenation of different activated ketones with the magnetic catalyst ($Pt/SiO_2/Fe_3O_4$) and with the Pt/Al_2O_3 reference catalyst. Major enantiomer is indicated in parentheses.

Substrate	ee% $Pt/SiO_2/Fe_3O_4$	ee% Pt/Al_2O_3
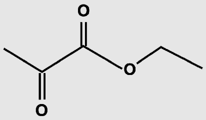	76 (R)	77 (R)
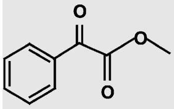	80 (R)	92 (R)
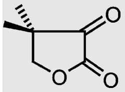	57 (R) 75[a] (R)	59 (R) 77[a] (R)
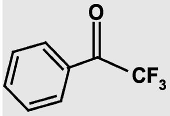	31 (R)	34 (R)

[a] Reaction performed at a hydrogen pressure of 100 bar.

Pt catalyst is rather surprising. It has been shown earlier [25] that even Pt catalysts based on the same support material, like e.g. Al_2O_3, but prepared from different precursors, show tremendous changes in the catalytic performance, particularly in enantioselectivity. It should be noted that the values of ee here reported were not optimized. Optimization of the reaction conditions can easily lead to an increase of the enantiomeric excess, as it has been previously shown [19,26–28]. In the present study we were interested in the comparison of the novel magnetic catalyst with the commercial Pt/Al_2O_3 under the same reaction conditions, therefore no further optimization has been done. Nonetheless, as a simple example of the sensitivity of the ee to the reaction conditions, in the hydrogenation of ketopantolactone (KPL) the ee improved to 75–77% for both the magnetic and the commercial catalyst when the hydrogen pressure was increased to 100 bar. Toluene was used for the tests of enantioselective hydrogenation with the novel magnetic catalyst since it is known that for the selected substrates and with the commercial Pt/Al_2O_3 catalyst the reaction in toluene gives among the highest ee values. Only for ethyl pyruvate better results were obtained using acetic acid instead of toluene as a solvent [19]. We additionally tested the magnetic catalyst using acetic acid as solvent, however, lower enantiomeric excess values than in the case of toluene were obtained for all the reported substrates. Furthermore intolerable iron leaching into solution occurred (>10 wt% of initial iron content in 2 h) ruling out the use of this medium when applying the magnetic Pt catalyst and indicating that some of the iron oxide was accessible.

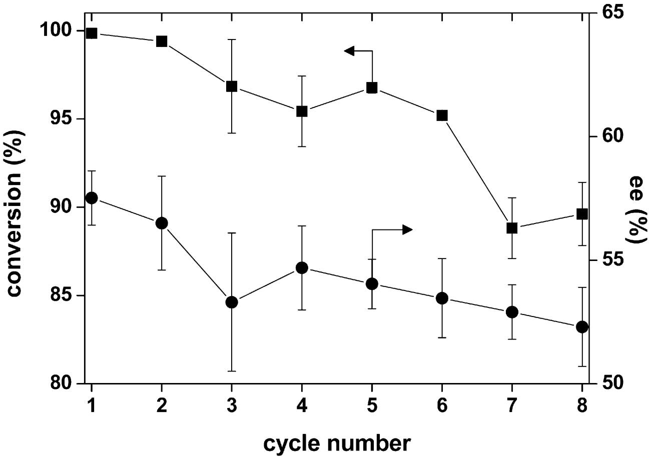

Fig. 7. Recyclability of the magnetic $Pt/SiO_2/Fe_3O_4$ catalyst. Conversion of KPL and enantiomeric excess of (*R*)-pantolactone in a series of subsequent reaction–separation steps. Experimental conditions are specified in Section 2.

The recycling properties of the magnetic catalyst were studied in detail for the hydrogenation of KPL in toluene. After each reaction cycle the catalyst was magnetically separated from the solution (Fig. 6), washed twice with toluene and reused without further activation. The enantioselectivity only slightly decreased from ee = 57% of the first run to a final value of ee = 52% after the eighth reaction cycle (Fig. 7). Under the conditions used, which are those typically reported for this class of reactions, the conversion was always 100% for a reaction time of 30 min. In order to study the change of activity after recycling the amount of catalyst was reduced, the concentration of the substrate was doubled and the reaction was interrupted after 14 min for each cycle. Fig. 7 shows that the conversion only slowly decreased for each cycle giving a loss of only 10% after the eighth cycle.

Possible leaching effect of Pt was studied by separating the supernatant solution from the catalyst after 3 min of reaction and allowing the hydrogenation to continue at 11 bar and for approximately 17 h in the solution without catalyst. The solution was periodically sampled and analyzed. The composition did not change during hydrogenation indicating that the supernatant solution was not catalytically active and that leaching of Pt, if present at all, was negligible. Additionally, potential leaching of iron was investigated by stirring the catalyst in the reaction solution with KPL and at a hydrogen pressure of 11 bar for 5 h which is comparable to the time required for eight hydrogenation cycles. In contrast to the experiments with acetic acid as solvent no significant amount of dissolved iron could be detected.

The hydrogenation reaction performed under standard conditions was also followed *in situ* via attenuated total reflection–infrared spectroscopy (ATR-IR) using a batch reactor mounted on an IR spectrometer. The IR spectrum of KPL shows a distinct band at 1800 cm^{-1} indicative of the carbonyl group which was hydrogenated during the reaction. Therefore the intensity change of this band was monitored in order to follow the reaction in real time. Since the background of the spectra was collected after introducing KPL in the reaction solution the spectra recorded during hydrogenation show a negative peak at 1800 cm^{-1} whose relative intensity increased in absolute value during the reaction (Fig. 8, inset). When the reaction was completed the intensity of the negative peak did not change further. Fig. 8 shows that for both, $Pt/SiO_2/Fe_3O_4$ and the Pt/Al_2O_3 reference catalyst, the reaction was completed in less than 15 min. In particular $Pt/SiO_2/Fe_3O_4$ showed even a faster conversion rate than the reference catalyst and most of the KPL was hydrogenated already during the first five minutes.

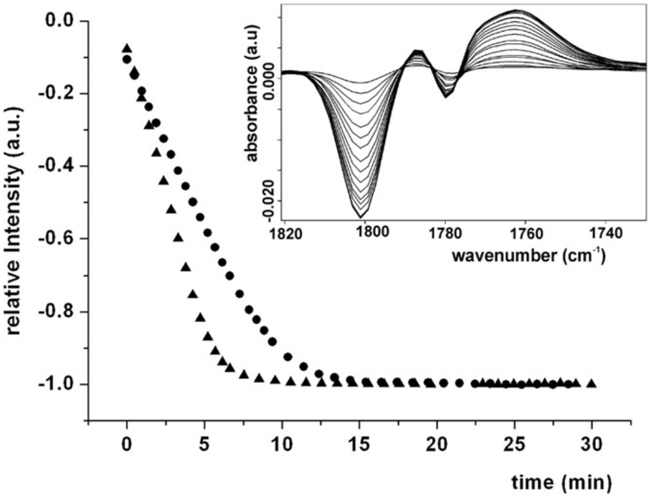

Fig. 8. Relative decrease of the carbonyl signal of KPL during hydrogenation using Pt/SiO_2/Fe_3O_4 (triangles) or Pt/Al_2O_3 (dots) as catalyst. The inset shows the spectrum of the relative decrease of the carbonyl stretching vibration band at 1800 cm^{-1}.

4. Conclusions

We have prepared a Pt-based magnetically separable catalyst for heterogeneous asymmetric hydrogenations using an easy synthetic route. The catalyst consisting of chirally modified Pt supported on Fe_3O_4 nanoparticles dispersed in a silica matrix shows similarly good catalytic performance in the hydrogenation of α-ketoesters and fluorinated ketones as the well-known commercial Pt/Al_2O_3 catalyst (Engelhard 4759) under the same conditions. The additional advantage of being superparamagnetic facilitates the separation, recovery and efficient reuse of the catalyst with almost complete retention of activity and enantioselective properties. The results here presented clearly show that supports bearing magnetic properties are convenient alternatives to traditional supports, such as alumina or silica, in the field of asymmetric hydrogenation on chirally modified platinum.

Acknowledgments

The authors are thankful to Dr. Frank Krumeich for the electron microscopy investigations performed at the electron microscopy center of ETH Zurich (EMEZ). We also thank Dr. Dagmar Goll and Lars Bommer from the Max-Planck-Institut für Metallforschung, Stuttgart (Germany) for the SQUID measurements and Fatos Hoxha and Dr. Cecilia Mondelli for fruitful discussions. Financial support by the Swiss National Foundation (Project 200020-113427) is kindly acknowledged.

References

[1] A.H. Lu, E.L. Salabas, F. Schüth, Angew. Chem. Int. Ed. 46 (2007) 1222.
[2] R.N. Grass, E.K. Athanassiou, W.J. Stark, Angew. Chem. Int. Ed. 46 (2007) 4909.
[3] G.M. Whitesides, C.L. Hill, J.-C. Brunie, Ind. Eng. Chem. Process Des. Dev. 15 (1976) 226.
[4] P.D. Stevens, G. Li, J. Fan, M. Yen, Y. Gao, Chem. Commun. (2005) 4435.
[5] A.H. Lu, W. Schmidt, N. Matoussevitch, H. Bönnemann, B. Spliethoff, B. Tesche, E. Bill, W. Kiefer, F. Schüth, Angew. Chem. Int. Ed. 43 (2004) 4303.
[6] S.C. Tsang, V. Caps, I. Paraskevas, D. Chadwick, D. Thompsett, Angew. Chem. Int. Ed. 43 (2004) 5645.
[7] K.M. Yeo, S.I. Lee, Y.T. Lee, Y.K. Chung, I.S. Lee, Chem. Lett. 37 (2008) 116.
[8] M. Shokouhimehr, Y. Piao, J. Kim, Y. Jang, T. Hyeon, Angew. Chem. Int. Ed. 46 (2007) 7039.
[9] R. Abu-Reziq, D. Wang, M. Post, H. Alper, Adv. Synth. Catal. 349 (2007) 2145.
[10] J.M.J. Jacinto, P.K. Kiyohara, S.H. Masunaga, R.F. Jardim, L.M. Rossi, Appl. Catal. A Gen. 338 (2008) 52.
[11] D.K. Yi, S.S. Lee, J.Y. Ying, Chem. Mater. 18 (2006) 2459.
[12] A. Hu, G.T. Yee, W.B. Lin, J. Am. Chem. Soc. 127 (2005) 12486.
[13] T. Mallat, E. Orglmeister, A. Baiker, Chem. Rev. 107 (2007) 4863.
[14] M. Bartók, Curr. Org. Chem. 10 (2006) 1533.
[15] M. Heitbaum, F. Glorius, I. Escher, Angew. Chem. Int. Ed. 45 (2006) 4732.
[16] H.U. Blaser, B. Pugin, F. Spindler, J. Mol. Catal. A Chem. 231 (2005) 1.
[17] T. Mallat, S. Diezi, A. Baiker, in: G. Ertl, H. Knözinger, F. Schüth, J. Weitkamp (Eds.), Handbook of Heterogeneous Catalysis, vol. 7, Wiley–VCH, 2008, pp. 3603–3626.
[18] X.Q. Liu, Z.Y. Ma, J.M. Xing, H.Z. Liu, J. Magn. Magn. Mater. 270 (2004) 1.
[19] S.M. Schürch, O. Schwalm, T. Mallat, J. Weber, A. Baiker, J. Catal. 169 (1997) 275.
[20] A. Baiker, J. Mol. Catal. A Chem. 115 (1997) 473.
[21] P. Tartaj, T. González-Carreño, C.J. Serna, Adv. Mater. 13 (2001) 1620.
[22] A.P. Philipse, M.P.B. Vanbruggen, C. Pathmamanoharan, Langmuir 10 (1994) 92.
[23] M.L.Z.-H. Qin, Y.-N. Sun, S. Shaikhutdinov, H.-J. Freund, J. Phys. Chem. C 112 (2008) 10209.
[24] M. von Arx, T. Mallat, A. Baiker, Tetrahedron: Asymmetry 12 (2001) 3089.
[25] J.T. Wehrli, A. Baiker, D.M. Monti, H.U. Blaser, J. Mol. Catal. 61 (1990) 207.
[26] B. Török, K. Balázsik, M. Török, Gy. Szöllösi, M. Bartók, Ultrason. Sonochem. 7 (2000) 151.
[27] M. von Arx, T. Mallat, A. Baiker, J. Catal. 193 (2000) 161.
[28] K. Szőri, K. Balázsik, K. Felföldi, M. Bartók, J. Catal. 241 (2006) 149.